Yoko Shibata, Jim F. White, Maria J. Serrano-Vega, Francesca Magnani, Amanda L. Aloia, Reinhard Grisshammer and Christopher G. Tate
Thermostabilization of the neurotensin receptor NTS1
Journal of Molecular Biology, 2009; 390(2):262-277

Originally published at:
http://doi.org/10.1016/j.jmb.2009.04.068

doi:10.1016/j.jmb.2009.04.068 J. Mol. Biol. (2009) 390, 262–277

JMB

Available online at www.sciencedirect.com

ScienceDirect

ELSEVIER

Thermostabilization of the Neurotensin Receptor NTS1

Yoko Shibata[1], Jim F. White[2], Maria J. Serrano-Vega[1], Francesca Magnani[1], Amanda L. Aloia[2], Reinhard Grisshammer[2]* and Christopher G. Tate[1]*

[1]*MRC Laboratory of Molecular Biology, Hills Road, Cambridge CB2 0QH, UK*

[2]*Membrane Protein Structure and Function Unit, National Institute of Neurological Disorders and Stroke, National Institutes of Health, Department of Health and Human Services, Rockville, MD 20852, USA*

Received 29 January 2009; received in revised form 27 April 2009; accepted 29 April 2009
Available online 5 May 2009

Structural studies on G-protein-coupled receptors have been hampered for many years by their instability in detergent solution and by the number of potential conformations that receptors can adopt. Recently, the structures of the β_1 and β_2 adrenergic receptors and the adenosine A_{2a} receptor were determined in the antagonist-bound state, a receptor conformation that is thought to be more stable than the agonist-bound state. In contrast to these receptors, the neurotensin (NT) receptor NTS1 is much less stable in detergent solution. We have therefore used a systematic mutational approach coupled with activity assays to identify receptor mutants suitable for crystallization, both alone and in complex with the peptide agonist NT. The best receptor mutant NTS1-7m contained four point mutations. It showed increased stability compared to the wild-type receptor, in the absence of ligand, after solubilization with a variety of detergents. In addition, NTS1-7m bound to NT was more stable than unliganded NTS1-7m. Of the four thermostabilizing mutations, only one residue (A86L) is predicted to be in the lipid environment. In contrast, I260A appears to be buried within the transmembrane helix bundle, F342A may form a distant part of the putative ligand-binding site, whereas F358A is likely to be in a region that is important for receptor activation. NTS1-7m binds NT with a similar affinity for the wild-type receptor. However, agonist dissociation was slower, and NTS1-7m activated G-proteins poorly. The affinity of NTS1-7m for the antagonist SR48692 was also lower than that of the wild-type receptor. Thus, we have successfully stabilized NTS1 in an agonist-binding conformation that does not efficiently couple to G-proteins.

Keywords: membrane protein; G-protein-coupled receptor; conformational thermostabilization

Edited by J. Bowie

Introduction

Determination of membrane protein structures has long been regarded as a difficult area in structural biology. To obtain diffraction-quality crystals, a target membrane protein needs to be available in sufficient quantities, stable in detergent solution from which crystallization occurs, and obtainable in one particular conformation. Stability in a range of detergents is central to crystal formation, but other factors such as removal of flexible protein parts or choice of the crystallization system (vapor diffusion or lipid-based approaches) may also need to be considered.[1] Increasing successes with bacterial membrane proteins, such as transporters and ion channels, have shown that many of the perceived difficulties in membrane protein crystallization can now be overcome. The first membrane protein struc-

**Corresponding authors.* E-mail addresses: rkgriss@helix.nih.gov; cgt@mrc-lmb.cam.ac.uk.

Abbreviations used: NT, neurotensin; GPCR, G-protein-coupled receptor; β_2AR, β_2 adrenergic receptor; A_{2a}R, adenosine A_{2a} receptor; β_1AR, β_1 adrenergic receptor; CHS, cholesteryl hemisuccinate; TM, transmembrane; [^{3}H]-NT, [^{3}H]-neurotensin; wt-NTS1, wild-type neurotensin receptor; DDM, *n*-dodecyl-β-D-maltopyranoside; Chaps, 3-[(3-cholamidopyropyl) dimethylammonio]-1-propanesulfonate; MBP, maltose-binding protein; LBA, ligand binding assay; DM, *n*-decyl-β-D-maltopyranoside; NG, *n*-nonyl-β-D-glycopyranoside; GDP, guanosine 5′-diphosphate; GTPγS, guanosine 5′-*O*-[γ-thio]triphosphate; ECL3, extracellular loop 3; PDB, Protein Data Bank; EDTA, ethylenediaminetetraacetic acid.

tures solved were all rigid, stable proteins and came from natural sources: a photosynthetic reaction center[2] and an outer membrane porin[3] from bacteria, and the bovine cytochrome *c* oxidase[4] and bc_1 complex[5] from mitochondria. More recently, eukaryotic membrane proteins from heterologously expressed sources have also been crystallized (e.g., the rat Kv1.2 voltage-gated potassium channel expressed in *Pichia pastoris*[6] and a chicken acid-sensing ion channel expressed in insect cells).[7]

One commonality between eukaryotic membrane proteins, whose structures have been solved, may be their relative stability in detergent—a consideration that also applies to many prokaryotic membrane proteins. Unfortunately, a direct comparison of the stabilities of all membrane proteins in detergents in which they have been crystallized has not been carried out. However, many successful crystallization conditions, especially for eukaryotic membrane proteins, included ligands, lipids, and/or lipid-like compounds, with the aim of improving the stability of a particular membrane protein during crystallization. If stability in detergent is one of the key determinants of crystallizability, then solving structures of a large number of human membrane proteins may currently not be possible because solubilizing these proteins in detergent would inactivate them.

Attempts to determine the structures of G-protein-coupled receptors (GPCRs) have been ongoing for over 20 years. Bovine rhodopsin was the first GPCR to be crystallized,[8–10] reflecting its relatively high stability in many detergents as long as the receptor was kept in its inactive, dark state. Many other GPCRs have been overproduced in a variety of expression systems,[11] and some of them have been purified to homogeneity. However, it has only been recently that structures have been determined for the human β_2 adrenergic receptor (β_2AR)[12,13] and the human adenosine A_{2a} receptor (A_{2a}R)[14] using the T4 lysozyme fusion strategy and lipidic cubic-phase crystallization procedures, while the structure of a thermostabilized β_1 adrenergic receptor (β_1AR) was determined from crystals grown in detergent by vapor diffusion.[15] The β_2AR was also crystallized in complex with an antibody fragment using the bicelle system.[16] These recent successes are due partly to increased usage of microfocus beamlines to collect X-ray diffraction data from very small crystals, but also due to our understanding of how to maintain receptors in a biologically relevant single conformation long enough for crystallization to occur. This was achieved by inclusion, during crystallization, of high-affinity antagonists/inverse agonists (β_2AR, β_1AR, and A_{2a}R) or cholesteryl hemisuccinate (CHS) (β_2AR and A_{2a}R), all of which are predicted to improve the stability of the receptor during crystallization.[14,17–20] Receptor stability has also been improved by site-directed mutagenesis (β_1AR), which allowed the use of more denaturing short-chain detergents for crystallization.[19] Insertion of the T4 lysozyme fusion partner into the flexible third cytoplasmic loop of receptors appears to improve the crystallizability of the receptor (β_2AR and A_{2a}R),[12,14] although the effect of T4 lysozyme on the stability of the receptor is unknown.

We now know the structures of five GPCRs (β_2AR, β_1AR, A_{2a}R, bovine rhodopsin, and squid rhodopsin[21]) in an inactive antagonist-bound state and the structure of one GPCR (bovine opsin) in an active-like state.[22,23] Although the structures of antagonist-bound GPCRs show great similarities within transmembrane (TM) cores, there are also differences, especially in the conformations of extracellular and intracellular loops, such that it is not yet possible to predict in atomic detail how, for example, a specific ligand binds to a receptor of unknown structure. β_1AR, β_2AR, and A_{2a}R bind small ligands within the TM core, and their structures in the antagonist-bound states are similar to the structure of dark-state rhodopsin. However, larger ligands such as peptides involve receptor regions other than the TM bundle for binding, and agonist-bound receptors, regardless of the sizes of their ligands, are thought to be much more flexible and/or to undergo rapid equilibrium between multiple structural states.[24] Therefore, the agonist-bound activated states of peptide receptors are still an unknown territory in GPCR structures.

We have focused our attention on a peptide receptor, the neurotensin (NT) receptor NTS1.[25] NT is a 13-amino-acid peptide agonist that is thought to bind in an extended conformation[26] to the receptor at a site formed by both extracellular loops and TM helices, as predicted from mutagenesis and structure–activity studies combined with modeling techniques.[27,28] The agonist-binding site overlaps with that of the antagonist SR48692, although the small synthetic antagonist requires only the TM helices for its binding.[29] Extensive work on the expression and purification of NTS1 has led to the production of milligram quantities of a highly purified functional receptor from *Escherichia coli*,[30] but diffraction-quality crystals have not yet been obtained. NTS1 is not particularly stable in detergent; it requires the presence of CHS and glycerol throughout purification to retain ligand-binding activity, and its stability in short-chain detergents is severely compromised. We therefore decided to identify thermostabilizing NTS1 mutants to allow the use of a wider range of detergents and buffer conditions for crystallization. Such a mutagenesis approach has successfully identified mutations in both bacterial membrane proteins[31,32] and GPCRs,[18,19] and conformational thermostabilization of the β_1AR in an antagonist-bound form[19] was essential for its subsequent structure determination at 2.7 Å resolution.[15] One constraint that we imposed upon the stabilization procedure was that NTS1 needed to be stabilized ideally in both the unliganded state and the NT-bound state because this would allow rapid purification of the mutated receptor using a well-established automated procedure.[30] Here we describe the successful thermostabilization of

NTS1 in both the unliganded state and the NT-bound state.

Results

Development of thermostability assays for the NT receptor

An essential prerequisite to our thermostabilization strategy is to develop a robust thermostability assay for the unpurified detergent-solubilized receptor based upon radioligand binding.[18,19] In this instance, the thermostability of NTS1 was determined using a [^{3}H]−neurotensin ([^{3}H]-NT; [3,11-tyrosyl-3,5-^{3}H(*N*)]pyroGlu-Leu-Tyr-Glu-Asn-Lys-Pro-Arg-Arg-Pro-Tyr-Ile-Leu) binding assay. To directly compare the stability of wild-type neurotensin receptor (wt-NTS1) with that of β_1AR, wt-NTS1 was solubilized, and its thermostability was determined in a buffer system similar to that used for β_1AR, containing only *n*-dodecyl-β-D-maltopyranoside (DDM).[19] However, the apparent T_m in DDM was rather low with limited reproducibility, possibly because solubilized unliganded wt-NTS1 was too unstable and therefore was sensitive to fluctuations in laboratory temperature (results not shown). To improve the reproducibility of thermostability assays, 3-[(3-cholamidopyropyl) dimethylammonio]-1-propanesulfonate (Chaps), CHS, and glycerol at final concentrations of 0.6%, 0.12%, and 30%, respectively, were included during the solubilization in 1% DDM, conditions that had previously been found to be highly stabilizing.[33] The concentration of NaCl in the thermostability assay was kept as low as possible (27 mM in the assay buffer, carried over from the lysis buffer), as a high concentration of Na^+ is known to inhibit NT binding to the receptor.[34,35] The concentration of [^{3}H]-NT used in the assays (12 nM) was at least fivefold above the apparent K_d value for detergent-solubilized wt-NTS1 (K_d = 1–2 nM in this buffer condition; results not shown) to allow high receptor occupancy, but it kept nonspecific [^{3}H]-NT binding to a minimum. Under these conditions, wt-NTS1 showed apparent T_m values of 24±2 °C in the unliganded state and 37±2 °C with NT bound (Fig. 1a). The apparent T_m was defined as the temperature at which 50% of the solubilized receptor remained functional after incubation for 30 min.

In designing the thermostabilization strategy for NTS1, we also considered how the receptor was going to be purified and the most likely state in which we would want to crystallize it. Crystallization is best performed under conditions where the receptor is most stable; NTS1 should therefore be crystallized with NT bound, as suggested by the thermostability assay (Fig. 1a). However, the purification scheme for NTS1 relies upon a ligand affinity purification step using an NT-affinity column.[30] Therefore, the ideal NTS1 construct for structural studies would be stable in both the presence and the absence of NT. With this in mind,

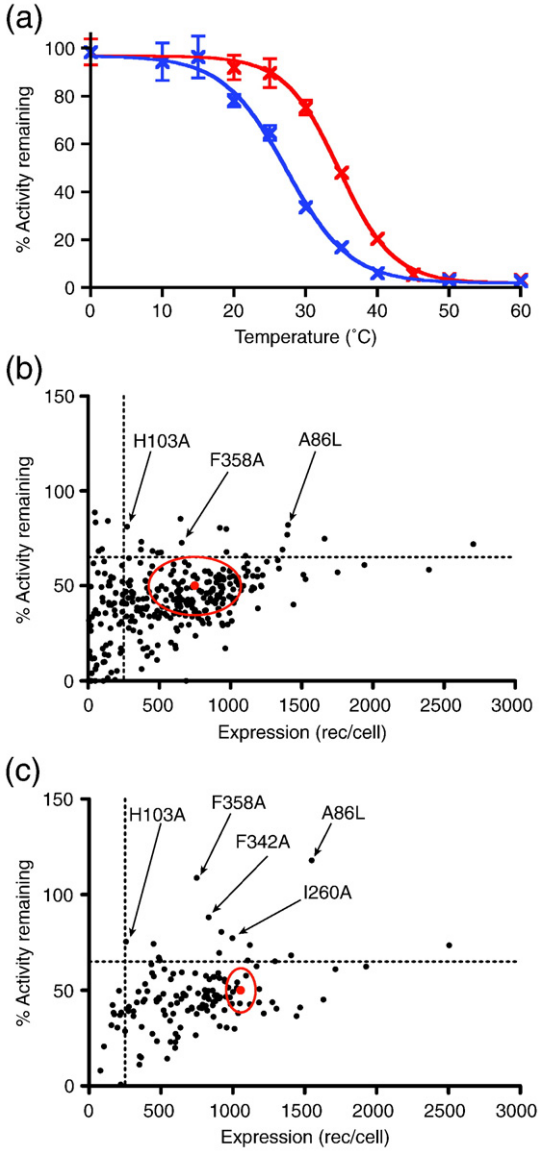

Fig. 1. Thermal stability and expression levels of NTS1 single Ala/Leu mutants. (a) The thermal stability of wt-NTS1 in the unliganded state (blue) and with NT bound (red) was assessed by determining the apparent T_m value from the midpoint of the curves. Apparent T_m of unliganded wt-NTS1, 24±2 °C; apparent T_m of NT-bound wt-NTS1, 37±2 °C. (b and c) Individual mutants of NTS1, each containing a single alanine mutation (if the original amino acid was alanine, then it was mutated to leucine), are summarized for its expression level in *E. coli* (number of functional receptors per cell), its thermal stability in the absence of NT (b), and in the presence of NT (c). Thermal stability was measured after incubating each detergent-solubilized mutant at 24 °C (b) or 37 °C (c) for 30 min, and the percentage of activity remaining after incubation was determined with respect to its own unheated control. All stability data are normalized against wt-NTS1 stability for each set of experiments (wt = 50%). The mean wt-NTS1 expression level and stability (red dot) and standard errors (red oval) are shown in the plots. The dotted lines show the cutoff values for the stabilized mutants (65% activity remaining, 250 receptors/cell).

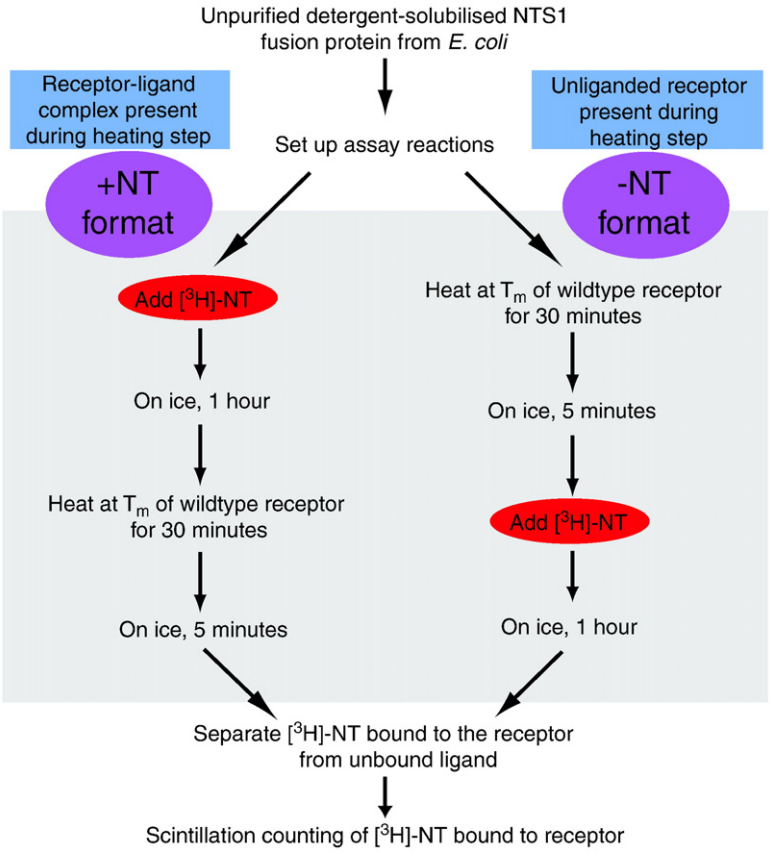

Fig. 2. Schematic of the "+NT" and "−NT" thermostability assays.

we developed two thermostability assay formats for detergent-solubilized NTS1, which we refer to as "−NT assay" and "+NT assay" (Fig. 2). In the −NT assay, solubilized NTS1 was heated at apparent T_m without a ligand (24 °C; Fig. 1a) for 30 min and placed on ice. [^{3}H]-NT was then added and, after a 1-h incubation on ice, the amount of [^{3}H]-NT bound to the receptor was determined by using a mini gel-filtration spin column to separate the receptor–ligand complex from free [^{3}H]-NT. In the +NT assay, the 30-min heating step at 37 °C (apparent T_m with NT bound; Fig. 1a) was performed *after* the addition of [^{3}H]-NT. Thus, the −NT assay determined the stability of the unliganded receptor, and the +NT assay determined the stability of the NT-bound NTS1.

Screening Ala/Leu scan mutants for thermostability in the unliganded state

We made 340 point mutations throughout NTS1 from Ile61 to Thr400 and expressed them as maltose-binding protein (MBP) fusions in *E. coli*. Three hundred eleven positions were mutated to alanine, and 29 native alanine residues were changed to leucine. Western blot analyses of whole-cell lysates probed with anti-MBP antibody showed similar intensities of bands corresponding to the NTS1 fusion protein (within threefold of the wild-type expression level) for all mutants, except for C142A and C225A. These cysteine residues are predicted to form a disulfide bond, and mutating either one of them led to a dramatic reduction in the expression levels of the full-length fusion proteins and increased proteolysis (results not shown). [^{3}H]-NT ligand binding assays (LBAs) performed on detergent-solubilized receptors at 4 °C revealed that 50 mutants, including C142A and C225A, did not bind an agonist possibly because the respective NTS1 mutants were misfolded or because a given mutation reduced agonist affinity directly or indirectly such that [^{3}H]-NT binding could not be detected at the ligand concentration used in the assay. Thermostability assays were performed on each of the 290 functional mutants. The assays were performed first in the −NT assay format to determine the stability of unliganded detergent-solubilized NTS1 mutants. The percentage of the remaining functional receptor was determined by comparing the amount of bound [^{3}H]-NT after heating with its unheated control. As the percentage of active wt-NTS1 remaining after heating varied between 30% and 50%, mutant values were scaled to values expected if the wt-NTS1 activity remaining was 50%, thus allowing a direct comparison between different batches of data. The accumulated error estimated for the activity assays, when expressed as the number of receptors per cell, was ±15%. In summary, out of all 340 NTS1 mutants constructed, 22 (6%) showed an improvement in stability (i.e., greater than 65% of functional receptors remaining after the incubation for 30 min at 24 °C) (Fig. 1b). In contrast, 201 mutants (59%)

retained a stability similar to that of wt-NTS1 in the unliganded state (~35% to 65% activity remaining after heating), 67 mutants (20%) were less stable than wt-NTS1, and 50 mutants (15%) did not bind NT (as mentioned above). The positions of the 22 best thermostabilizing mutations of NTS1 in the absence of ligand (Fig. 3b, blue and green) neither conform to an obvious pattern nor correspond to the locations of thermostabilizing mutations identified in β_1AR[19] or A_{2a}R.[18]

Most of the thermostabilized mutants retained at least 50% of the total number of functionally expressed receptors per cell compared to wt-NTS1 (Fig. 1b). However, we also observed exceptions. For example, the mutation H103A stabilized the unliganded receptor by 7–8 °C, but expression of H103A was nearly fourfold lower than that of wt-NTS1, making this mutant less attractive for further use. In order to improve the expression level, five other amino acid residues, namely, H103N, H103S, H103V, H103L, and H103M, were used to substitute this residue. Of these five mutants, H103N and H103S expressed at the same level as wt-NTS1, while H103V showed only a slight improvement in expression over H103A; all three mutations maintained the thermostability conferred by H103A. In contrast, H103L and H103M neither regained the expression level of wt-NTS1 nor retained the thermostability of H103A (data not shown). Although it was not necessary to use any of these additional changes in subsequent mutants, these data show that the low expression level of a functional thermostable receptor can be improved by changing the thermostabilizing mutation to different amino acid residues.

The best thermostabilizing mutations of the NTS1 unliganded state for combination into an optimally stable receptor were chosen only after considering their effect upon NTS1 expression. We considered that 250 functional receptors per *E. coli* cell (about 25% of wt-NTS1 expression) represented the minimum acceptable level of expression and, using this as our cutoff, 19 of 22 NTS1 mutants were retained

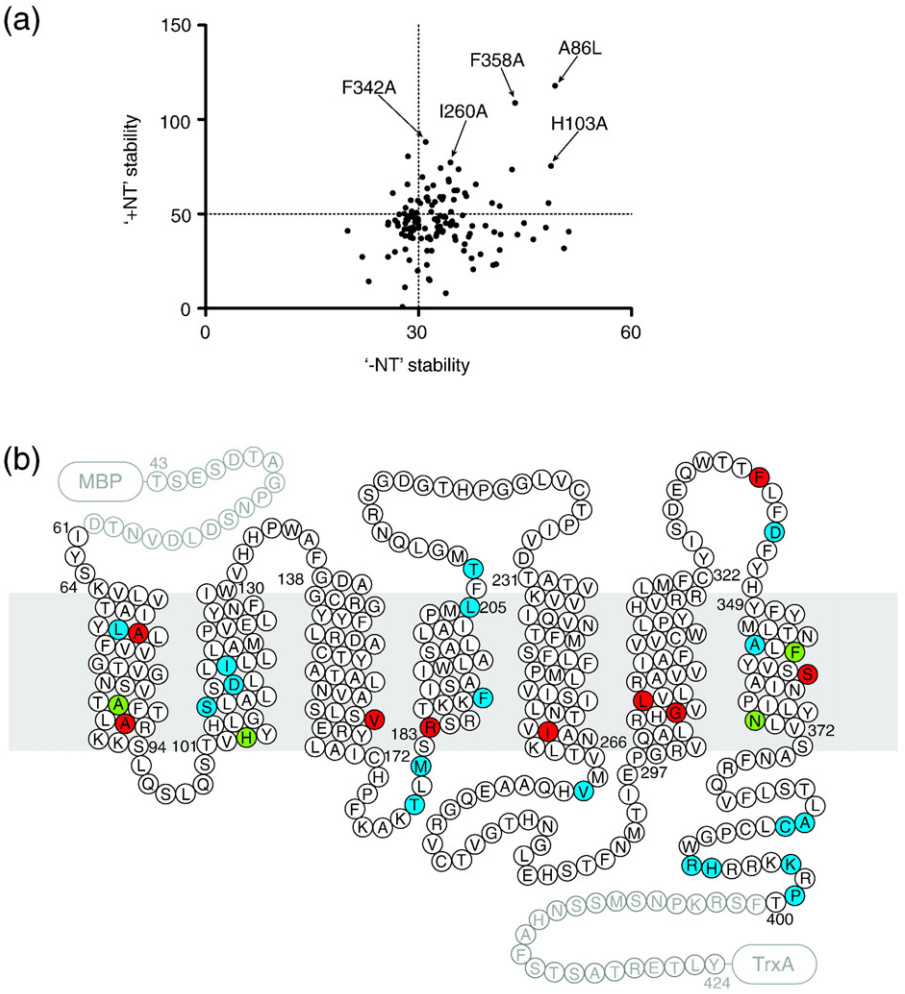

Fig. 3. Comparison of the unliganded-state and agonist-bound-state stabilities of NTS1 single Ala/Leu mutants. (a) The stability of each mutant is shown in both the unliganded state (−NT stability) and the agonist-bound state (+NT stability). Mutations combined to optimally stabilize NTS1 are indicated. The intersection of dotted lines in the plot corresponds to the position of wt-NTS1. (b) The locations of 31 stabilizing mutations are shown in the snake plot; positions of stabilizing mutations are shown for the unliganded receptor (blue), NT-bound receptor (red), or both (green).

for the subsequent study. Each of these stabilizing mutations gave an increase in the apparent T_m value in the unliganded state of 2–10 °C, compared to wt-NTS1 (Supplementary Table 1).

Rescreening Ala/Leu scan mutants for thermostability in the NT-bound state

All 22 thermostabilizing Ala/Leu single mutants selected in the unliganded state (−NT assay) were subsequently tested for thermostability in the NT-bound state (+NT assay). To our surprise, many of the mutants were less stable than wt-NTS1 when bound to NT, although they were clearly more stable than wt-NTS1 in the unliganded state (data not shown). In fact, 7 of the 22 mutants were less stable in the +NT assay than wt-NTS1 (Supplementary Table 1). Therefore, we decided to reanalyze the mutants that retained >50% activity (i.e., at least as stable as wt-NTS1) in the −NT assay. Thus, 137 mutants were detergent-solubilized and heated in the presence of [^{3}H]-NT at 37 °C for 30 min (+NT assay; Fig. 2). Only 13 of 137 mutants screened were found to be more stable than wt-NTS1 in the NT-bound state (cutoff value set to ~65%). There appeared to be little correlation between the stability of the mutants in the unliganded state and the stability of the mutants in the NT-bound state (Fig. 3a), and there was no discernable pattern from the positions of the mutations in the primary amino acid sequence (Fig. 3b, red and green). The 13 mutants chosen by the NT assay were, from the selection strategy we imposed, more stable than wt-NTS1 in the NT-bound state and at least as stable as wt-NTS1 in the unliganded state, and 11 of the 13 mutants also expressed reasonably well (Supplementary Table 1). Each of the stabilizing mutations had apparent T_m values of 1–7 °C higher than that of wt-NTS1 in the NT-bound state. Only four mutants were more stable than wt-NTS1 in both the unliganded state and the NT-bound state, of which only three mutants, namely, A86L, H103A, and F358A, were significantly more stable (Fig. 3b, green). The denaturation profiles of these three mutants and wt-NTS1 are shown in Fig. 4, in the absence (Fig. 4a) and in the presence (Fig. 4b) of bound [^{3}H]-NT, and the apparent T_m values are shown in Fig. 4c.

Combining mutations to further improve receptor stability

To evolve an NTS1 mutant that was stable both in the presence and in the absence of NT, we chose 14 single mutations that stabilized the unliganded state (from the −NT assay) and another 13 mutations that stabilized the NT-bound state (from the +NT assay), including the 4 mutations that appeared in both groups. Mutants that were significantly less stable than wt-NTS1 in the NT-bound state (e.g., L72A) and/or had low expression levels (e.g., D345A) (Supplementary Table 1) were not used. Combinations within subsets of mutations were obtained by

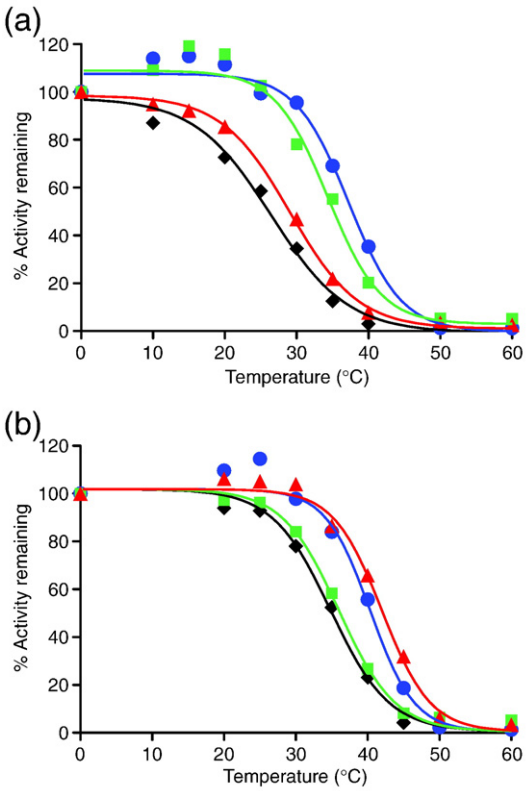

(c)

	-NT assay		+NT assay	
	T_m (°C)	ΔT_m (°C)	T_m (°C)	ΔT_m (°C)
wt	27	-	35	-
A86L	37	10	39	4
H103A	34	7	36	1
F358A	29	2	42	7

Fig. 4. Denaturation profiles of the three best NTS1 single Ala/Leu mutants in the absence and in the presence of NT. Denaturation curves of the three best thermostable single mutants of NTS1 (A86L, H103A, and F358A) were determined by heating the solubilized mutants at elevated temperatures for 30 min, either in the absence of NT (a) or in the presence of 12 nM [^{3}H]-NT (b). The NTS1 mutants shown are wild type (black diamonds), A86L (blue circles), H103A (green squares), and F358A (red triangles). (c) Table summarizing the apparent T_m values determined by nonlinear regression of the above curves; constraint of upper–lower boundaries was not used. The estimated error from repeated experiments is ±2 °C. Remaining activity was normalized to 100% based upon the amount of binding measured in the samples incubated on ice.

PCR using random mixtures of primers, as previously described for the thermostabilization of β_1AR[19] and A_{2a}R.[18] The most thermostable mutants contained combinations of the five mutations A86L, H103A, I260A, F342A, and F358A (Supplementary Table 2). Most of these mutants also maintained reasonably good expression levels, with many showing improved levels of expression over wt-NTS1. The assay conditions had to be revised at this point by increasing the incubation temperatures (to 37 °C for the '−NT' assay and to 47 °C for the '+NT' assay) to ensure better differentiation in the degree

of stabilization between mutants. Under these conditions, wt-NTS1 showed no binding activity, so results were normalized to A86L, which retained about 20% of its initial activity in both assay formats (Fig. 5). Among the 26 mutant combinations tested, 6 combinations showed improved thermostability in the absence of NT (score >30), and 11 combinations showed improved thermostability in the presence of NT (score >80) over the respective stability of A86L (Supplementary Table 2). Mutants containing both A86L and F358A mutations appeared to show the best stabilization effects in both screening conditions. NTS1-7a, which contains only two mutations (A86L and F358A), gave more than 10 °C stabilization compared to wt-NTS1 in both +NT and −NT formats (Fig. 5). NTS1-7m (A86L, I260A, F342A, and F358A) was found to be one of the most thermostable mutants, with an apparent T_m of 50 °C in the presence of NT (13 °C better than wt-NTS1; Fig. 5) and an apparent T_m of 42 °C in the absence of NT (17 °C better than wt-NTS1; Fig. 5).

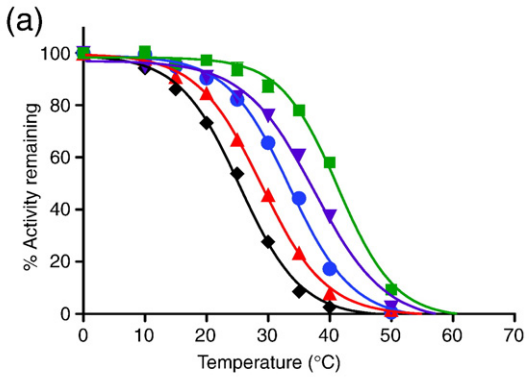

(c)

	-NT assay		+NT assay	
	T_m (°C)	ΔT_m (°C)	T_m (°C)	ΔT_m (°C)
wt	25	-	37	-
A86L	33	8	40	3
F358A	28	3	45	8
NTS1-7a	36	11	47	10
NTS1-7m	42	17	50	13

Fig. 5. Denaturation profiles of NTS1 multiple mutants in the absence or in the presence of NT. Denaturation curves of four examples of the best thermostable mutants—NTS1-7a (A86L/F358A), NTS1-7m (A86L/I260A/F342A/F358A), A86L, and F358A—were compared to wt-NTS1. The solubilized receptors were heated for 30 min, either in the absence (a) or in the presence (b) of NT: wt-NTS1 (black diamonds), A86L (blue closed circles), F358A (red triangles), NTS1-7a (purple inverted triangles), and NTS1-7m (green squares). (c) Table summarizing the apparent T_m values determined from the above curves. The estimated error from repeated experiments is ±2 °C. Remaining activity was normalized to 100% based upon the amount of binding measured in the samples incubated on ice.

Ligand binding properties of thermostable NTS1 mutants

To define the effects of mutations on the ligand binding properties of mutant receptors, the apparent K_d values for agonist ([^{3}H]-NT) binding were determined by saturation binding assays using intact *E. coli* cells expressing wt-NTS1 or selected mutants. Competition binding curves for the displacement of [^{3}H]-NT by the antagonist SR142948 were used to determine K_i values for its binding. Seven mutants that showed good stabilization in one or both +NT and −NT assays and reasonable expressions levels were tested (Fig. 6). All the thermostabilized NTS1 mutants had an apparent K_d for NT binding that was either similar to that of wt-NTS1 (K_d = 0.27 nM on intact *E. coli* cells) or slightly better (Fig. 6). K_d values of NT for the mutants varied between 0.03 nM for NTS1-7o and 0.22 nM for NTS1-7l. In contrast, the affinities of NTS1 mutants for the antagonist SR142948 varied from near-wild-type values of 0.22 nM for NTS1-7o to 2.8 nM for NTS1-7g when determined in competition with [^{3}H]-NT (Fig. 6). When the K_i (SR146948):K_d(NT) ratio was determined, then all the mutants tested, with the exception of NTS1-7l, showed preferential binding to NT compared to SR146948 by a factor of up to 18 for NTS1-7f.

Characterization of NTS1-7m

NTS1-7m satisfied our original aim of stabilizing NTS1 in both unliganded and NT-bound states. In addition to the thermal denaturation profiles of detergent-solubilized NTS-7m (Fig. 5), we determined the degree of thermostabilization by measuring the rate of thermal inactivation at 45 °C for detergent-solubilized wt-NTS1 and NTS1-7m (Fig. 7a). Under the conditions used, the half-lives for NTS1-7m were either 220 or 13.4 min, in the presence or in the absence of bound NT, respectively, compared to values of 5.7 and 1.3 min for wt-NTS1. Based on these half-lives, NT-bound NTS1-7m was 39-fold more stable than NT-bound wt-NTS1 and was 10-fold more stable when the unliganded receptors were compared.

Thermostabilization of β_1AR and A_{2a}R in DDM resulted in both these receptors gaining stability in short-chain detergents that are more denaturing but more suitable for crystallization.[18,19] We therefore tested whether NTS1-7m that was thermostabilized in DDM/Chaps/CHS showed increased stability in other detergents that are more preferable for crystallization. NTS1-7m and wt-NTS1 were solubilized in

DDM/Chaps/CHS, bound to Ni^2-affinity resin, and washed with either DDM/Chaps/CHS (the original detergent condition), 0.03% DDM, 0.1% *n*-decyl-β-D-maltopyranoside (DM), or 0.3% *n*-nonyl-β-D-glycopyranoside (NG). The receptors were eluted in the desired detergents, and thermal denaturation profiles were determined by heating the receptors in the presence of [^{3}H]-NT (Fig. 7b and c). NTS1-7m was consistently more stable than wt-NTS1 in any of the detergents tested, with apparent T_m values that were 7–13 °C higher than those of the wild-type receptor. As expected, the stability of NTS1-7m decreased as the size of the detergent micelle around the receptor also decreased, reflecting the increasing harshness of detergents (DDM<DM<NG) with shorter hydrophobic chains. The amount of functional receptor eluted from the Ni^2-NTA column was also consistently higher for NTS1-7m than for wt-NTS1 [e.g., washing and eluting the receptors in NG recovered only 3% of the functional wt-NTS1 compared to 20% for NTS1-7m (compared to values determined in DDM/Chaps/CHS)]. Although NTS1-7m was consistently more stable in short-chain detergents than wt-NTS1, the degree of stabilization was less than that observed in DDM/Chaps/CHS (Fig. 7d).

To investigate what might contribute to the stability of NTS1-7m, the rate of agonist dissociation from detergent-solubilized receptors (in 0.1% DDM, 0.2% Chaps, and 0.04% CHS) was determined (Fig. 8a). In this detergent condition, the K_d values of NTS1-7m and wt-NTS1 are 0.66 and 1.1 nM (results not shown). Although the exact K_d values depend on the concentrations of the detergents used, the relative orders in the affinity of mutant NTS1s and wt-NTS1 are unchanged. The dissociation rate of NT from wt-NTS1 in the presence of NaCl is 50-fold higher than that in the absence of the salt (Fig. 8a). On the other hand, the effect of NaCl on the dissociation rate was only ~2-fold for NTS1-7m. Therefore, the off-rate of NT from wt-NTS1 was ~8-fold faster than that from NTS1-7m in the absence of NaCl; however, in the presence of 0.8 M NaCl, the off-rate of NT from wt-NTS1 was over 200-fold faster than that from NTS1-7m (Fig. 8a).

The ability of NTS1-7m to couple to the G-protein $G\alpha q\, G\beta_1\gamma_1$ was tested in a guanosine 5′-diphosphate (GDP)/guanosine 5′-*O*-[γ-thio]triphosphate (GTPγS) exchange assay performed on receptors expressed in insect cell membranes using the baculovirus expression system. The *E. coli* and insect cell expression systems both produce NTS1 with equivalent NT binding activities, but the *E. coli* system

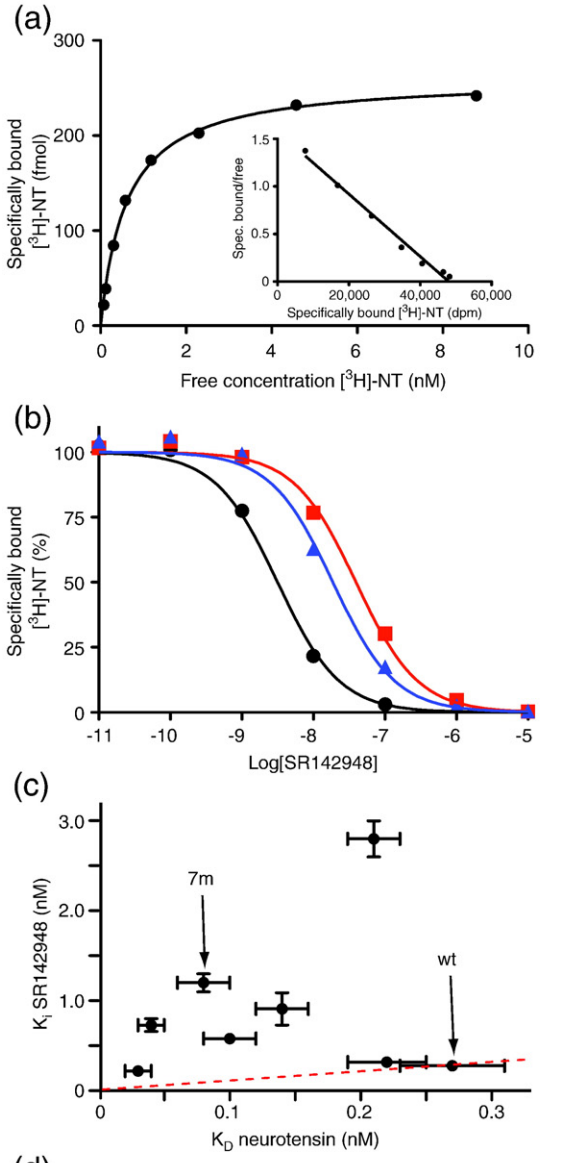

(d)

Receptor	K_D neurotensin (nM)	K_i SR142948 (nM)	Ratio K_i : K_D
wt-NTS1	0.27 ± 0.04	0.28 ± 0.01	1.0
NTS1-7a	0.10 ± 0.02	0.58 ± 0.04	5.8
NTS1-7e	0.14 ± 0.02	0.91 ± 0.18	6.5
NTS1-7f	0.04 ± 0.01	0.73 ± 0.07	18
NTS1-7g	0.21 ± 0.02	2.8 ± 0.2	13
NTS1-7l	0.22 ± 0.03	0.32 ± 0.03	1.5
NTS1-7m	0.08 ± 0.02	1.2 ± 0.1	15
NTS1-7o	0.03 ± 0.01	0.22 ± 0.02	7.3

Fig. 6. Agonist and antagonist binding to NTS1 mutants. (a) Saturation binding curve of a representative [^{3}H]−NT binding experiment with NTS1-7m in intact *E. coli* cells. The Scatchard plot is shown as an inset (one-site fit; $K_d = 0.34 \pm 0.03$ nM). (b) Competition assays were performed using intact *E. coli* cells expressing either wt-NTS1 or NTS1 mutants. Increasing quantities of antagonist SR142948 were incubated with the cells in the presence of 5 nM agonist [^{3}H]−NT. Competition curves for wt-NTS1 (black circles), NTS1-7a (blue triangles), and NTS1-7m (red squares) are shown. K_i values were determined by nonlinear regression analyses using K_d values for NT binding determined from the saturation binding curves (d). (c) The correlation between K_d(NT) and K_i(SR142948) for each mutant is shown as a scatter plot, with results of a representative experiment shown and with error bars representing the SEM of data fitting. The red broken line represents the K_i/K_d ratio for wt-NTS1. (d) Table summarizing the apparent K_d values for [^{3}H]−NT binding, K_i values for SR142948, and the K_i/K_d ratio for each of the mutants tested. K_d and K_i determinations were performed simultaneously, in duplicate, for each mutant. SEMs are obtained from one representative experiment and arise from data fitting.

requires the presence of N-terminal and C-terminal fusion proteins (MBP and TrxA, respectively) for high-level expression. As TrxA at the C-terminus could affect G-protein coupling, untagged NTS1 and NTS1-7m were therefore expressed in insect cells for the G-protein coupling assays. Although robust agonist-induced nucleotide exchange at Gαq was seen for wt-NTS1, only poor coupling was observed for NTS1-7m (Fig. 8b).

Discussion

The rat NT receptor NTS1 was an obvious target for thermostabilization because NTS1 is not very stable in detergent solution, especially in short-chain detergents that are potentially useful for three-dimensional crystallization. Heterologous expression of NTS1 in *E. coli* and purification of functional receptors have been well established by White *et al.*[30] An essential step during the purification of NTS1 is the use of an NT ligand-affinity column, which allows enrichment of functional receptors. The application of NTS1 onto the NT column requires that no ligand is present at this time; therefore, this dictated that NTS1 should be stabilized in the unliganded state to improve its stability during the steps before binding to the NT column. As crystallization would likely involve the cocrystallization of NTS1 with NT, it was also desirable that stabilized NTS1 would be at least equally stable in the presence of bound agonist as in the unliganded state. These two criteria governed the approach for the stabilization procedure.

The identification and combination of thermostabilizing point mutations were performed by an Ala/Leu scanning methodology that had previously been used to stabilize both β_1AR and A_{2a}R. Out of the 31 best thermostabilizing point mutations identified in NTS1 by the −NT and +NT assays, the combination of the four mutations A86L, I260A, F342A, and F358A produced one of the most thermostable mutants developed so far, NTS1-7m. NTS1-7m displayed several modified properties compared to wt-NTS1, including the following: an increase in the thermostabilities of the solubilized unpurified form (Fig. 5) and the partially purified form, as well as an increase in thermostability in short-chain detergents (Fig. 7); a decrease in the NT dissociation rate (yet similar apparent NT affinity) and a smaller effect of Na^+-induced NT dissociation (Fig. 8a); a decrease in antagonist affinity (Fig. 6); and reduced ability to functionally couple to Gαq

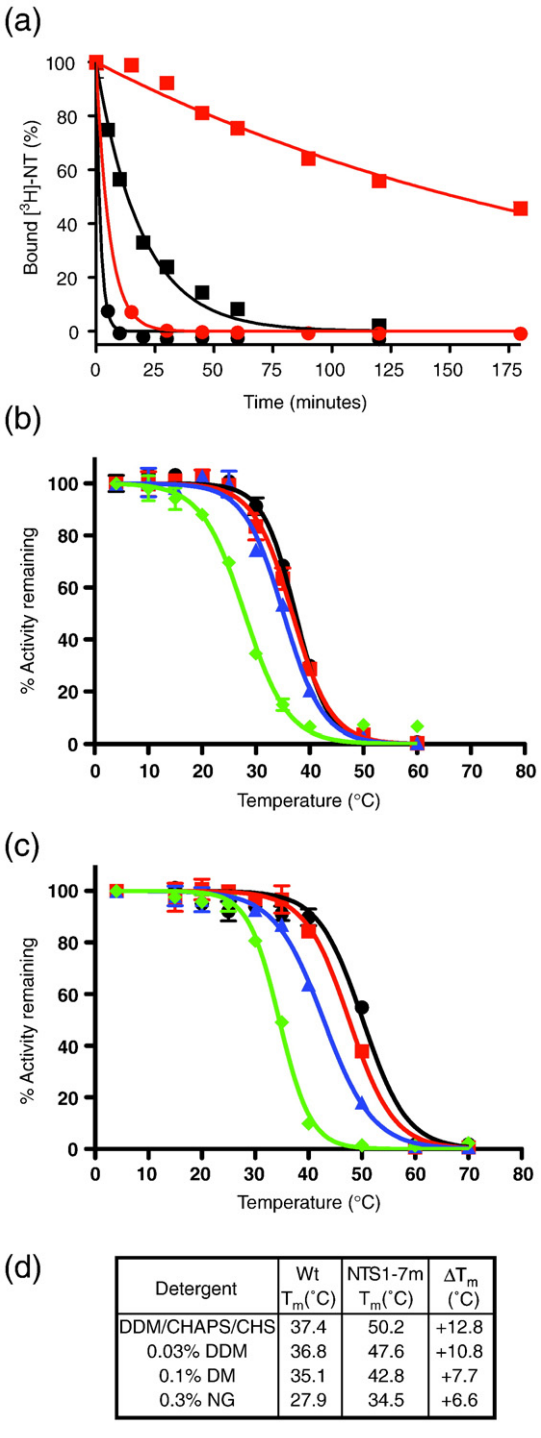

(d)

Detergent	Wt T_m(°C)	NTS1-7m T_m(°C)	ΔT_m (°C)
DDM/CHAPS/CHS	37.4	50.2	+12.8
0.03% DDM	36.8	47.6	+10.8
0.1% DM	35.1	42.8	+7.7
0.3% NG	27.9	34.5	+6.6

Fig. 7. NTS1-7m shows improved thermal stability and stability in short-chain detergents compared to wt-NTS1. (a) The rates of thermal inactivation of solubilized wt-NTS1 (circles) and NTS1-7m (squares) in DDM/Chaps/CHS were compared by heating the samples at 45 °C either in the presence (red lines) or in the absence (black lines) of [^{3}H]−NT. Half-lives were determined from the curves by nonlinear regression of the single-exponential curve after constraining the values for Y=0–100% and plateau=0%: unliganded wt-NTS1, 1.3 min; NT-bound wt-NTS1, 5.7 min; unliganded NTS1-7m, 13.4 min; NT-bound NTS1-7m, 220 min. (b–d) Thermostability of wt-NTS1 and NTS1-7m in various detergents. Receptors were solubilized in DDM/Chaps/CHS, bound to Ni^2-NTA beads, and then washed and eluted with a buffer containing either DDM/Chaps/CHS (black circles), 0.03% DDM (red squares), 0.1% DM (blue triangles), or 0.3% NG (green diamonds). Thermostability assays were performed in the presence of NT (b: wt-NTS1; c: NTS1-7m). Remaining activity was normalized against the unheated control in each detergent condition (100%), although recovery yields were different in each case (see the main text). The apparent T_m values (d) were determined from the curves by nonlinear regression.

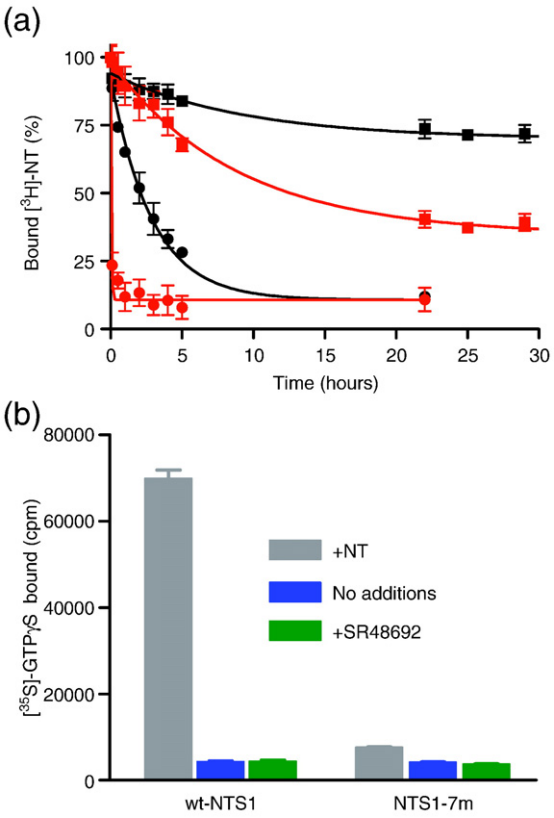

Fig. 8. Rate of dissociation of NT and activation of G-protein by wt-NTS1 and NTS1-7m. (a) The dissociation rates of [^{3}H]-NT from wt-NTS1 (circles) and NTS1-7m (squares) were determined by quantifying the amount of [^{3}H]-NT remaining bound to the receptors (total NT concentration in the assay, 2 nM) upon addition of 50 μM unlabeled NT on ice in the presence (red) or in the absence (black) of NaCl. The rate of [^{3}H]-NT dissociation was determined by nonlinear regression with single-exponential decay. (b) Recombinant receptors in urea-washed insect cell membranes were tested for their ability to stimulate G-protein using a GDP/[^{35}S]−GTPγS exchange assay. All assays contained purified recombinant Gαq $G\beta_1\gamma_1$, [^{35}S]−GTPγS, and insect cell membranes containing either wt-NTS1 or NTS1-7m. Receptors were incubated with no additional ligands (blue bars), with NT (grey bars), or with the antagonist SR48692 (green bars). The amount of [^{35}S]−GTPγS bound to the G-protein complex was determined as described in the text.

$G\beta_1\gamma_1$ (Fig. 8b). While it would be convenient to associate each of these properties with a single mutation within the receptor, it is likely that the combined effect of all the four mutations in NTS1-7m generates the overall characteristics of the mutant. For the purposes of this discussion, however, each property of NTS1-7m will be discussed in terms of how individual and/or combined mutations within NTS1-7m may contribute to its observed characteristics.

Several three-dimensional structural models were made by overlaying the position of NTS1 amino acid primary sequence to bovine rhodopsin and β_1AR-m23 crystal structures according to amino acid sequence alignment (Fig. 9, shown in the β_1AR-m23 structure). The residue A86 is located in TM1; the equivalent amino acid side chains in the structures of β_2AR (I55),[12] β_1AR (I63),[15] rhodopsin (L59),[8,9] and A_{2a}R (C28)[14] all make contact with the lipid environment, but also with TM2. Based on the above receptor structures, the I260 side chain in TM5 is predicted to point towards the (D/E)RY motif in TM3. F342 is located in extracellular loop 3 (ECL3) and is likely to be able to interact with residues known to form the ligand-binding pocket. F358 is in TM7 and may interact with a conserved tryptophan residue in TM6 (position 6.48[36]) that is thought to be part of the "toggle switch" for receptor activation.[37]

Binding of NT is clearly one of the important factors governing the stability of NTS1, even for the wild-type receptor. NT binding to the thermostable mutant NTS1-7m differed in several ways from binding to wt-NTS1, although the K_d values for binding were similar. The rate of dissociation of NT from NTS1-7m was 8-fold slower than that for wt-NTS1. However, the rate of NT dissociation was only affected by about 2-fold by the presence of 0.8 M NaCl, compared to an acceleration of dissociation by over 50-fold for wt-NTS1. In contrast, the affinity of the antagonist SR142948 for NTS1-7m was reduced by ~4-fold. The binding site for NT was predicted to include the region of ECL3;[27,38,39] thus, the F342A mutation of NTS1-7m may be of importance in regard to its modified agonist-binding properties. While F342 has not previously been reported as being directly involved in NT binding, the ECL3 location of F342 places it within the region of the predicted receptor-agonist-binding pocket, and modeling studies have implicated F342 in NT binding through its contribution to the aromatic character of the ligand-binding pocket.[39]

The binding of antagonists to NTS1-7m was consistently weaker compared to binding to wt-NTS1, whether it was measured as a K_i value from competition binding experiments between SR142948 and [^{3}H]-NT (4-fold weaker binding; Fig. 6) or by a saturation binding assay using [^{3}H]−SR48692 (15-fold weaker binding; data not shown). A reduced affinity of antagonist binding has been previously observed for F358A-mutated NTS1.[40] Mutational studies, combined with binding assays using SR48692 and its analogues, have predicted π–π interactions between the dimethoxyphenyl group of the ligand and F358 of the receptor. SR48692 has additional predicted contacts at M208, F331, R327, Y324, Y351, T354, and Y359 of the receptor, none of which is mutated in NTS1-7m.

In addition to the observed decrease in the NT off-rate, binding of NT to NTS1-7m was also not modulated by Na^+ similarly to wt-NTS1 (Fig. 8a). Like other rhodopsin-like GPCRs, NTS1's affinity for its agonist is influenced by the presence of Na^+, with a decrease in the apparent NT affinity being observed with increasing Na^+ concentration.[34] The Na^+ effect can be eliminated by the mutation of a highly conserved aspartic acid residue in TM2 to an uncharged residue (D113A).[34] The equivalent residue D83 in bovine rhodopsin, for example, is

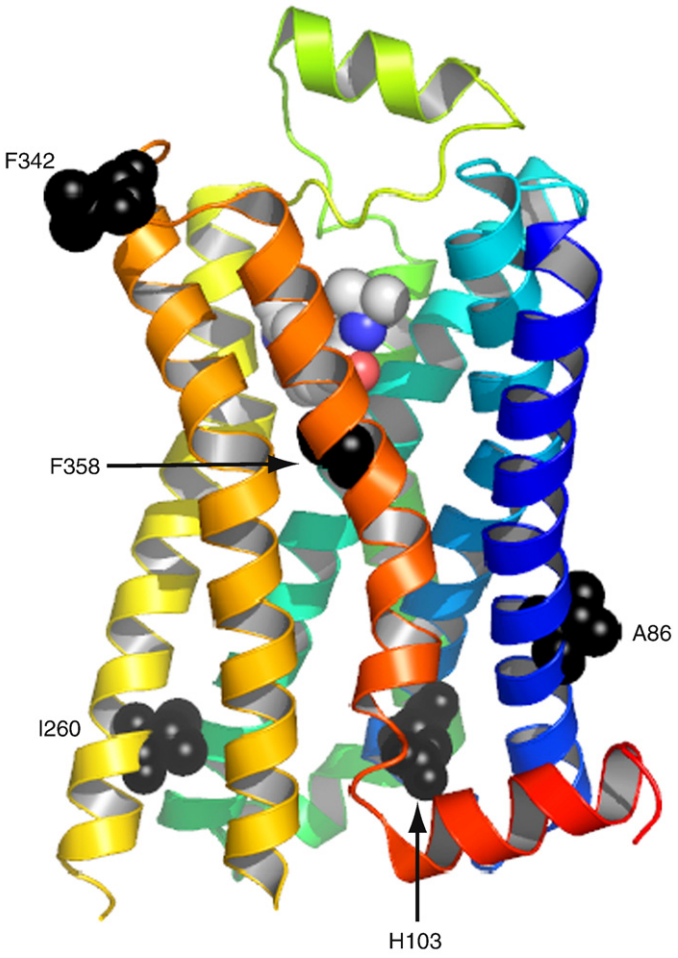

Fig. 9. Positions of thermostabilizing mutations in NTS1-7m. The structure of the β_1AR (PDB ID 2VT4) is shown in rainbow colors (N-terminus in blue; C-terminus in red), with the bound antagonist cyanopindolol shown as a space-filling model. The equivalent positions (via primary amino acid sequence alignment) of five thermostabilizing mutations of NTS1 are shown, with side chains as space-filling models (black) and with labels corresponding to the amino acid residues in NTS1.

involved in an extensive H-bond network that has been suggested to contribute to the stability and function of this receptor.[9] How the Na^+ effect has been largely abolished by mutations in NTS1-7m, none of which lie in TM2, remains unclear, nor is it obvious whether the Na^+ effect observed with NTS1-7m relates to the Na^+ effect involving D113.

While our primary purpose was to thermostabilize the receptor in various detergents, it is interesting to determine whether the mutant NTS1-7m could assume the activated (R*) conformation to couple to G-proteins, either in the absence or in the presence of NT. To our surprise, NTS1-7m did not efficiently catalyze nucleotide exchange at Gαq (Fig. 8b), either in the absence or in the presence of NT, even though NT could clearly bind to the receptor. This was unexpected because one of the thermostabilizing mutations was F358A, which has been previously shown to promote constitutive activity of NTS1,[41] so our expectation was to observe some constitutive activity of NTS1-7m in addition to agonist-induced G-protein coupling activity. Disruption of the intrahelical salt bridge ("ionic lock") of the conserved (D/E)RY motif in TM3 is important for GPCR activation, and mutations within this motif have been associated with the constitutive activity of GPCRs.[24,42] In this regard, the I260A mutation, in combination with the F358A mutation, of NTR1-7m may be playing a part. Sequence alignment[36] of rat NTS1 with turkey β_1AR, human β_2AR, human A_{2a}R, and bovine rhodopsin places I260 of NTR1 at V230 (β_1AR), V222 (β_2AR), I200 (A_{2a}R), and L226 (rhodopsin). These hydrophobic side chains point towards the main-chain atoms of the (D/E)RY tyrosine in the crystal structures of these receptors [Protein Data Bank (PDB) IDs 2VT4, 2RH1, 3EML, and 1GZM]. It may be that removal of the isoleucine side chain in the NTS1 mutation I260A in some way counteracts the expected constitutively activating effect of the F358A mutation, as well as the ability to assume agonist-induced activated conformations.

The four mutations in NTS1-7m clearly have had an effect on the global conformation of the receptor. This is evident from the improved thermostability of NTS1-7m and the inability of NT-bound NTS1-7m to couple to G-proteins efficiently. Only one of the four thermostabilizing mutations could possibly interact with NT based upon current models, suggesting that the other three mutations in combination affect the pharmacology of NTS1-7m through indirect effects. In the absence of a crystal structure, we cannot definitively say what conformation NTS1-7m has; however, given the G-protein coupling data, when NT is bound, it is not an activated state of the receptor.

One aim of producing NTS1-7m was to provide a mutant that is suitable for purification by the sequential use of Ni^2-NTA resin and an NT column[30] and that is more stable than wt-NTS1. While the stability of solubilized NTS1-7m was improved compared to that of wt-NTS1 (i.e., beneficial during the initial step of receptor purification), the use of the NT column was not successful. This is largely because the off-rate of NT from NTS1-7m in the presence of high NaCl concentrations is considerably slower than that for wt-NTS1. NTS1-7m binds to an NT column, but it cannot be eluted using high-concentration (e.g., 1 M) NaCl; therefore, the NT column step in its present form is no longer an effective tool for purification. If we were to continue using the established purification procedures, further work on mutagenesis efforts to stabilize NTS1 with different sets of mutations will be required. Otherwise, a new purification scheme would need to be developed before crystallization can be attempted with NTS1-7m.

Recently, a study by Sarkar *et al.* describing the evolution of NTS1 for expression and stability was published.[43] This approach was based on random mutagenesis by error-prone PCR, expression of the mutant library in *E. coli*, and identification of the most highly expressing mutants by a fluorescence-activated cell sorter after binding a fluorescent NT analogue. This procedure identified the mutant D03, which contains nine mutations (H103D, H105Y, A161V, R167L, R213L, V234L, H305R, S362A, and S417C) located in TM2, TM3, ECL2, TM6, TM7, and the C-terminus. The NTS1 mutant D03 expressed almost 10-fold better in *E. coli* than wt-NTS1, and it appeared 3- to 4-fold more stable than wt-NTS1 in detergent at 45 °C (based on replotting of the data in Fig. 5 of Sarkar *et al.*[43]). This work assumed that there was a correlation between expression levels and stability, but mutagenesis work on the β_1AR,[19] A_{2a}R,[18] and NTS1 reported here (Fig. 1) shows that stability and expression levels are only weakly correlated. Because of this, our approach to selecting the best receptor construct was based on choosing the most stable mutants regardless of their expression levels. Indeed, we found NTS1-7m to be 10-fold more stable at 45 °C in detergent solution (in the absence of NT; Fig. 7), with an expression level (less than 2-fold improvement) similar to that of wt-NTS1. In addition, this stabilization effect was achieved by having only four mutations in NTS1-7m compared with nine mutations (excluding silent mutations) in the mutant D03. The most stabilizing conditions that we observed for NTS1-7m were in the presence of bound NT; under these conditions, NTS1-7m was 39-fold more stable than wt-NTS1, but equivalent figures for the mutant D03 are not available. One interesting finding in the mutant D03 was that its NT binding is also insensitive to Na^+ concentration. Unlike NTS1-7m, however, D03 does contain mutations in TM2 near D113, as well as residues in TM3, which may be in contact with D113. Again, without a crystal structure, it is difficult to suggest how this effect has arisen.

We have now successfully applied the approach of conformational thermostabilization to three GPCRs: NTS1 (this work), A_{2a}R,[18] and β_1AR.[19] In all cases, the receptor is stabilized in a conformation that preferentially binds either agonist or antagonist, depending upon which ligand was used during the selection procedure. Currently, there are insufficient data to predict which mutation may be thermostabilizing, so an Ala/Leu scan coupled to thermostability assays is still the best way to proceed. Our data also show that the position of thermostabilizing mutations is different for each receptor, so it is likely that the transferability of thermostability between distantly related receptors is low. After producing the thermostabilized β_1AR mutant, the structure containing bound antagonist was determined to 2.7 Å resolution.[15] The intrinsic instability of agonist-bound wt-NTS1 compared to antagonist-bound wt-β_1AR suggested that more effort is needed to achieve an optimally stabilized NT receptor that is suitable for crystallization. Our work presented here shows that a systematic mutagenesis approach can be used to evolve a receptor that is thermostable both in the presence and in the absence of ligand. In addition, this selection strategy gave rise to mutant receptors that bind the agonist NT preferentially over antagonist SR142948, although the combination of two selection pressures on stability has resulted in a mutant receptor that virtually does not couple to G-proteins. A different approach will be required to stabilize the receptor in a fully activated state, which may require the selection of thermostable mutants in the presence of relevant G-proteins.

Materials and Methods

Materials

The tritiated agonist [^{3}H]-NT was purchased from Perkin Elmer. The tritiated antagonist [methoxy-^{3}H]−SR48692 {SR48692: {2-[(1-(7-chloro-4-quinolinyl)-5-(2,6-dimethoxyphenyl)pyrazol-3-yl)carbonylamino]tricyclo(3.3.1.1.$^{3.7}$)decan-2-carboxylic acid}} was purchased from Amersham Biosciences/GE Healthcare (discontinued in November 2007). Unlabeled NT was purchased from Sigma. The unlabeled antagonist SR142948 {2-[[[5-(2,6-dimethoxyphenyl)-1-[4-[[[3-(dimethylamino)propyl]methylamino]carbonyl]-2-(1-methylethyl)phenyl]-1*H*-pyrazol-3-yl]carbonyl]amino]-tricyclo[3.3.1.1$^{3.7}$]decan-2-carboxylic acid} was purchased from Tocris Bioscience (referred to as SR142948A in Gully *et al.*[44]). Detergents were purchased from the following suppliers: DDM (Glycon or Anatrace), DM (Anatrace), NG (Anatrace), Chaps (Anatrace), and CHS Tris salt (Sigma or Anatrace). Detergent concentrations are given as percent weight per volume (g/100 ml solution).

NTS1 constructs for expression in *E. coli* and insect cells

wt-NTS1 refers to the N-terminally truncated rat NT type I receptor starting at Thr43. The wild-type receptor or a mutant form of receptor was expressed in *E. coli* as a

fusion protein, with the *E. coli* MBP preceding the receptor N-terminus and a thioredoxin–decahistidine tag (TrxA-H_{10}) following the receptor C-terminus.[30,45] For the construction of recombinant baculoviruses, the cDNA sequences for wt-NTS1 and NTS1-7m were subcloned into the baculovirus transfer vector pFastBac1 (Invitrogen) without coding for the fusion partners at the N-terminus or C-terminus (Met-$NTS1_{T43\text{-}Y424}$).

Site-directed mutagenesis

Three hundred forty mutations were introduced throughout NTS1 from amino acid residues Ile61 to Thr400, spanning all seven TM helices, the putative helix 8, three intracellular and three extracellular loops, and the proximal half of the C-terminus, including potential phosphorylation sites. Each amino acid residue was changed to alanine, unless it was already an alanine in the wt-NTS1 sequence, at which time it was changed to leucine. Mutants were created by PCR-based site-directed mutagenesis using the *E. coli* expression plasmid as template and following the QuikChangeII methodology (Stratagene) but using KOD hot start polymerase (Novagen). The positions of helices were predicted by aligning the amino acid sequence of rNTS1 with those of three other type 1 GPCRs (bovine opsin, turkey β_1AR, and human A_{2a}R) and by superposing the alignment onto the known crystal structure of bovine rhodopsin (PDB ID 1GZM).[9] Individual clones were fully sequenced in the NTS1 coding region to ensure that only the desired mutation was present. Multiple mutations were introduced to the receptor by including up to four pairs (five pairs only in one case) of mutagenesis primers in a PCR, using a template already containing one mutation.

Expression of NTS1 in *E. coli* for screening of mutants

Expression of wt-NTS1 and NTS1 mutants was performed in *E. coli*,[30] with modifications. Cultures were grown in 50 ml of 2× TY supplemented with 100 μg/ml ampicillin and 0.2% glucose in 250-ml Erlenmayer flasks at 37 °C, with shaking to an OD_{600} of 0.5. After the addition of 0.5 mM IPTG, the temperature was lowered to 22 °C, and the cultures were incubated with shaking for another 24 h. Cultures were harvested as 2-ml aliquots by centrifugation at 13,000*g* for 1 min, flash-frozen in liquid nitrogen, and stored at −20 °C.

Radioligand binding and thermostability assays

Agonist binding to detergent-solubilized receptors was performed with [^{3}H]-NT.[30] The harvested *E. coli* cells expressing wt-NTS1 or mutant NTS1 were suspended in lysis buffer [50 mM Tris·HCl (pH 7.4), 200 mM NaCl, and 30% (vol/vol) glycerol] and supplemented with protease inhibitor cocktail (Roche), 0.75 mg/ml lysozyme, 25 μg/ml DNase I, 6.25 mM $MgCl_2$, 0.1% bovine serum albumin (BSA), and 0.004% bacitracin. Receptors were solubilized by adding 1% DDM, 0.6% Chaps, and 0.12% CHS (final volume, 500 μl). After centrifugation, the cleared lysate was used directly in LBAs in the assay buffer [50 mM Tris·HCl (pH 7.4), 1 mM ethylenediaminetetraacetic acid (EDTA), 0.1% BSA, 0.004% bacitracin, and 30% glycerol] containing detergents (0.22% DDM, 0.6% Chaps, and 0.12% CHS; final concentrations after addition of lysate) and 12 nM [^{3}H]-NT. The total number of functional receptors was determined by incubating the receptor in the assay buffer at 4 °C for 1 h in the presence of [^{3}H]-NT ('normal' LBA). Nonspecific binding of [^{3}H]-NT was assessed by either determining [^{3}H]-NT binding to wt-NTS1 in the presence of 4 μM unlabeled NT and/or performing LBA using DH5α cells not expressing any receptors in the presence or in the absence of 4 μM unlabeled NT. The amount of functional wt-NTS1 or mutant NTS1 (i.e., receptors retaining ligand binding) was determined by a 'spin assay.' A receptor–ligand complex was separated from free radioligand by applying the assay mixture on a spin column (QS-QM minicolumns, formerly supplied by Perkin Elmer and presently supplied by Fisher Scientific) packed with Sephadex G50 (GE Healthcare) preequilibrated in 50 mM Tris·HCl (pH 7.4), 1 mM EDTA, and 0.1% DDM. The receptor–ligand complex was eluted by centrifugation and analyzed by liquid scintillation counting (Beckman LS 6000).

Thermal stability was determined in the absence ('−NT' assay) or in the presence ('+NT' assay) of [^{3}H]-NT. In the −NT assay, neither ^{3}H-labeled nor unlabeled NT was present during incubation at 24 °C for 30 min. Samples were cooled on ice for 5 min, and then ligand was added ([^{3}H]-NT or [^{3}H]-NT/unlabeled NT), and the samples were incubated for an additional hour on ice. The amount of functional receptors after heating was determined by spin assay, as described above. In the +NT assay, the 30-min incubation at 37 °C was performed in the presence of [^{3}H]-NT or [^{3}H]-NT/unlabeled NT. Samples were cooled on ice then incubated on ice in the cold room for an additional hour before spin assay.

Saturation binding experiments were performed in the presence of 0.15–20 nM [^{3}H]-NT using detergent-solubilized receptors in LBA buffer. Nonspecific binding of NT to the receptor was determined by including 4 μM unlabeled NT. The apparent K_d values were obtained by nonlinear regression analysis using a one-site saturation binding with a ligand depletion model in Prism software (GraphPad).

Thermal denaturation curves were constructed by incubating solubilized receptors in the assay buffer in the absence (−NT) or in the presence (+NT) of 12 nM [^{3}H] −NT at eight different temperatures between 0 and 70 °C for 30 min. The samples were cooled on ice, and ligand was added to '−NT' assay mixtures. All the samples were subjected to spin assay after the 1-h incubation on ice. A potential change in nonspecific binding upon heating at extreme temperatures was initially tested by carrying out thermal denaturation experiments, including 4 μM unlabeled NT in the assays; no changes in nonspecific binding were seen after incubation at high temperatures. Data were analyzed by nonlinear regression using a Boltzmann sigmoidal model in the Prism software.

Denaturation time course of NTS1

To compare the stability of wt-NTS1 and mutant NTS1, the rate of thermal inactivation was tested by the decrease in activity over a period of time. NTS1 fusion proteins were solubilized, and +/−NT assays were prepared (as in thermostability assays) in large batches. Assay mixtures were aliquoted into eight equal amounts (~130 μl/tube) and heated at 45 °C in the presence or in the absence of [^{3}H]-NT. One tube was taken out of the incubator at eight different time points—0 (no incubation at 45 °C), 5, 10, 20, 30, 45, 60, and 120 min for −NT assays, and 0, 15, 30, 45, 60, 90, 120, and 180 min for NT assays and was plunge-cooled on ice for 5–10 min. The tritiated ligand [^{3}H]-NT was added to −NT assay samples. Samples were then incubated on ice for an additional hour before spin

assay. Solubilized receptors were also heated for 0 and 120 min (−NT) and for 0 and 180 min (+NT) at 45 °C in the presence of 4 μM unlabeled NT. No changes were observed in nonspecific binding after a long incubation. Data were analyzed by nonlinear regression using a one-phase exponential decay model in Prism software.

LBAs using intact *E. coli* cells

The frozen aliquots of cells expressing wt-NTS1 or mutant NTS1 were thawed on ice and resuspended in 1 ml of cold TEBB buffer [50 mM Tris·HCl (pH 7.4), 1 mM EDTA supplemented with 0.1% (wt/vol) BSA, and 0.004% bacitracin]. A 50-μl aliquot of cell mixture was used in a total volume of 500 μl of assay mixture (TEBB buffer and no detergents) containing 1 pM to 10 nM [^{3}H]-NT. Nonspecific binding of radioligand to the receptor was determined by including 4 μM unlabeled NT. The assay mixtures were incubated on ice for 2 h, and then applied to GF/B glass-fiber filters (Whatman) pretreated with polyethylenimine. The filters were washed three times with ice-cold TE (50 mM Tris, 1 mM EDTA, pH 7.4) buffer, dried, and counted in a Beckman LS 6000 scintillation counter. The apparent K_d values were obtained by nonlinear regression analysis using a one-site saturation binding with a ligand depletion model in Prism software.

The binding of the antagonist SR142948 to wt-NTS1 and mutant NTS1 was determined using the unlabeled antagonist SR142948 in a competition assay format. LBAs on intact *E. coli* cells were carried out at the [^{3}H]-NT concentration of 5 nM in the presence of 10 pM to 10 μM unlabeled antagonist. Assay samples were incubated on ice for 2 h, then the mixture was applied to GF/B filters as described above. Saturation binding experiments of the same NTS1 samples were carried out in parallel to determine the apparent K_d values. The apparent K_i values were determined by nonlinear regression analysis using a one-site competition model in Prism software.

Small-scale partial purification of NTS1 for stability tests in different detergents

The pellet from 100 ml of *E. coli* culture, expressing wt-NTS1 or mutant NTS1, was solubilized in 6 ml of lysis buffer [50 mM Tris·HCl (pH 7.4), 200 mM NaCl, and 30% (vol/vol) glycerol] containing 1% DDM, 0.6% Chaps, and 0.12% CHS. Five hundred microliters (50:50 slurry) of Ni^2-NTA agarose (Qiagen) pretreated with binding buffer [50 mM Tris·HCl (pH 7.4), 30% (vol/vol) glycerol, 50 mM imidazole, 100 mM NaCl, 0.1% DDM, 0.6% Chaps, and 0.12% CHS] was incubated with 1 ml of cleared lysate in the cold room with constant mixing for 1 h. The resin was washed once with 1 ml of binding buffer, then washed twice with 1 ml of wash buffer [50 mM Tris·HCl (pH 7.4), 30% (vol/vol) glycerol, 50 mM imidazole, 100 mM NaCl, and one of the desired detergents or the detergent combination (0.1% DDM/0.6% Chaps/0.12% CHS, 0.03% DDM, 0.1% DM, or 0.3% NG)]. The receptor was eluted from Ni^2-NTA resin using an elution buffer [50 mM Tris·HCl (pH 7.4), 30% (vol/vol) glycerol, 200 mM imidazole, 100 mM NaCl, and one of the desired detergents or the detergent combination]. Samples were subjected to spin assays. Thermostability was determined from denaturation profiles of the receptors in the desired detergent.

Dissociation of NT from detergent-solubilized NTS1

NTS1 fusion proteins were solubilized in a volume of 25 ml containing 5 g of wet *E. coli* cell paste, as described previously.[30] Receptors (0.7–0.8 nM) were incubated on ice for 2 h with [^{3}H]-NT (2 nM) in assay buffer [50 mM Tris·HCl (pH 7.4), 1 mM EDTA, 0.1% BSA, and 0.004% bacitracin] containing detergent (0.1% DDM, 0.2% Chaps, and 0.04% CHS). [^{3}H]-NT dissociation was then initiated by addition of 50 μM unlabeled NT or by addition of 50 μM NT and NaCl (833 mM). Samples were subjected to spin assays using Bio-Spin 30 Tris columns (Bio-Rad)[30] after the following incubation times: 0.1, 0.5, 1, 2, 3, 4, 5, and 22 h for wt-NTS1 (with and without NaCl), and after additional time points, 25 and 29 h, for NTS1-7m (with and without NaCl). The data were analyzed by nonlinear regression analysis using a one-phase exponential decay model in Prism software.

Expression of NTS1 in insect cells and preparation of P2 membranes

N-terminally truncated receptors (Met-NTS1$_{T43\text{-}Y424}$) (see NTS1 Constructs for Expression in *E. coli* and Insect Cells) were produced in *Trichoplusia ni* insect cells using the baculovirus expression system. Insect cells were infected at a multiplicity of infection of 5 and incubated for 48 h at 21 °C before harvest.

NTS1-enriched membranes were obtained as a P2 fraction from the insect cells essentially as described,[46] using a solution of 10 mM Mops (pH 7.5), 5 mM ethylene glycol bis(*b*-aminoethyl ether) *N*,*N*′-tetraacetic acid, and 100 μM 4-(2-aminoethyl)benzenesulfonyl fluoride HCl as lysis buffer. The P2 membranes were resuspended in lysis buffer containing 12% (wt/wt) sucrose, snap-frozen in liquid nitrogen, and stored at −80 °C.

Prior to G-protein coupling assays, the P2 membranes were treated with urea to remove peripherally bound membrane proteins.[47,48] The urea-stripped membranes were resuspended in 12% (wt/wt) sucrose containing Mops buffer (10 mM, pH 7.5), snap-frozen in liquid nitrogen, and stored at −80 °C. The receptor density in urea-washed P2 membranes was determined by [^{3}H]−NT saturation binding analysis. The samples were incubated for 1 h on ice in 0.5 ml of assay buffer [50 mM Tris·HCl (pH 7.4), 1 mM EDTA, 0.1% BSA, and 0.004% bacitracin]. Nonspecific [^{3}H]−NT binding was determined in the presence of 2 μM unlabeled NT. Separation of bound ligand from free ligand was achieved by rapid filtration through GF/B glass-fiber filters pretreated with polyethylenimine.

GDP/GTPγS exchange assay

Cephalopod Gαq was purified from dark-adapted retinas of *Sepia officinalis*, as described previously.[47] The dimer complex of Gβ$_1$ and Gγ$_1$ was purified from bovine retina.[49] The receptor-catalyzed exchange of GDP for GTPγS on Gαq was determined by modification of previously described procedures.[46,48] Reactions were carried out in 12 mm×75 mm siliconized borosilicate glass test tubes in a total assay volume of 50 μl. Urea-washed insect cell membranes containing wt-NTS1 or NTS1-7m were added to G-protein (Gαq Gβ$_1$γ$_1$) on ice to give a total volume of 30 μl. A reaction contained either the agonist NT or the nonpeptide antagonist SR48692,[50] or neither. GDP/GTPγS exchange was initiated by the addition of a 20-μl solution of [^{35}S]−GTPγS (Perkin Elmer). The final concentrations of the components in each reaction were as follows: 50 mM Mops (pH 7.5), 1 mM EDTA, 100 mM NaCl, 1 mM DTT, 3 mM $MgSO_4$, 0.3% BSA, 1 μM GDP, 4 nM [^{35}S]−GTPγS, 40 μM AppNHp, 0.4 mM

CMP, 1 nM receptor, 100 nM Gαq, 500 nM $G\beta_1\gamma_1$, and either 10 μM NT, 40 μM SR48692, or no ligand. The reaction mixtures were incubated at 30 °C for 5 min. Reactions were terminated by addition of 2 ml of ice-cold stop buffer [20 mM Tris·HCl (pH 8.0), 100 mM NaCl, and 25 mM $MgCl_2$]. The entire volume of each sample was filtered over a nitrocellulose membrane on a vacuum manifold. Filters were then washed six times with 2 ml of ice-cold stop buffer. The nitrocellulose membranes were dried overnight, and radioactivity was quantified by liquid scintillation in a Beckman LS 6500 scintillation counter.

Acknowledgements

This work was supported by a joint grant from Pfizer Global Research and Development and the MRCT Development Gap Fund, in addition to core funding from the MRC (Y.S., F.M., M.J.S.-V., and C.G.T.). The research work of J.F.W., A.L.A., and R.G. was supported by the Intramural Research Program of the National Institutes of Health, National Institute of Neurological Disorders and Stroke. We thank John K. Northup (National Institute on Deafness and Other Communication Disorders, National Institutes of Health, Department of Health and Human Services, Rockville, MD 20850, USA) for providing purified Gαq and $G\beta_1\gamma_1$. The production of NTS1 in insect cells was performed at the Protein Expression Laboratory, Advanced Technology Program, SAIC-Frederick, Inc., National Cancer Institute, Frederick, MD 21702, USA. DNA sequence analysis was performed by the National Institute of Neurological Disorders and Stroke DNA Sequencing Facility.

Supplementary Data

Supplementary data associated with this article can be found, in the online version, at doi:10.1016/j.jmb.2009.04.068

References

1. Warne, T., Serrano-Vega, M. J., Tate, C. G. & Schertler, G. F. (2009). Development and crystallization of a minimal thermostabilized G protein-coupled receptor. *Protein Expression Purif.* **65**, 204–213.
2. Deisenhofer, J., Epp, O., Miki, K., Huber, R. & Michel, H. (1985). Structure of the protein subunits in the photosynthetic reaction centre of *Rhodopseudomonas viridis* at 3 Å resolution. *Nature*, **318**, 618–624.
3. Weiss, M. S. & Schulz, G. E. (1992). Structure of porin refined at 1.8 Å resolution. *J. Mol. Biol.* **227**, 493–509.
4. Tsukihara, T., Aoyama, H., Yamashita, E., Tomizaki, T., Yamaguchi, H., Shinzawa-Itoh, K. *et al.* (1996). The whole structure of the 13-subunit oxidized cytochrome *c* oxidase at 2.8 Å. *Science*, **272**, 1136–1144.
5. Xia, D., Yu, C.-A., Kim, H., Xia, J.-Z., Kachurin, A. M., Zhang, L. *et al.* (1997). Crystal structure of the cytochrome *bc*1 complex from bovine heart mitochondria. *Science*, **277**, 60–66.
6. Long, S. B., Campbell, E. B. & Mackinnon, R. (2005). Crystal structure of a mammalian voltage-dependent Shaker family K channel. *Science*, **309**, 897–903.
7. Jasti, J., Furukawa, H., Gonzales, E. B. & Gouaux, E. (2007). Structure of acid-sensing ion channel 1 at 1.9 Å resolution and low pH. *Nature*, **449**, 316–323.
8. Palczewski, K., Kumasaka, T., Hori, T., Behnke, C. A., Motoshima, H., Fox, B. A. *et al.* (2000). Crystal structure of rhodopsin: a G protein-coupled receptor. *Science*, **289**, 739–745.
9. Li, J., Edwards, P. C., Burghammer, M., Villa, C. & Schertler, G. F. (2004). Structure of bovine rhodopsin in a trigonal crystal form. *J. Mol. Biol.* **343**, 1409–1438.
10. Standfuss, J., Xie, G., Edwards, P. C., Burghammer, M., Oprian, D. D. & Schertler, G. F. (2007). Crystal structure of a thermally stable rhodopsin mutant. *J. Mol. Biol.* **372**, 1179–1188.
11. Sarramegna, V., Talmont, F., Demange, P. & Milon, A. (2003). Heterologous expression of G-protein-coupled receptors: comparison of expression systems from the standpoint of large-scale production and purification. *Cell. Mol. Life Sci.* **60**, 1529–1546.
12. Cherezov, V., Rosenbaum, D. M., Hanson, M. A., Rasmussen, S. G., Thian, F. S., Kobilka, T. S. *et al.* (2007). High-resolution crystal structure of an engineered human beta2-adrenergic G protein-coupled receptor. *Science*, **318**, 1258–1265.
13. Hanson, M. A., Cherezov, V., Griffith, M. T., Roth, C. B., Jaakola, V. P., Chien, E. Y. *et al.* (2008). A specific cholesterol binding site is established by the 2.8 Å structure of the human beta2-adrenergic receptor. *Structure*, **16**, 897–905.
14. Jaakola, V. P., Griffith, M. T., Hanson, M. A., Cherezov, V., Chien, E. Y., Lane, J. R. *et al.* (2008). The 2.6 angstrom crystal structure of a human A_{2a} adenosine receptor bound to an antagonist. *Science*, **322**, 1211–1217.
15. Warne, T., Serrano-Vega, M. J., Baker, J. G., Moukhametzianov, R., Edwards, P. C., Henderson, R. *et al.* (2008). Structure of a beta1-adrenergic G-protein-coupled receptor. *Nature*, **454**, 486–491.
16. Rasmussen, S. G., Choi, H. J., Rosenbaum, D. M., Kobilka, T. S., Thian, F. S., Edwards, P. C. *et al.* (2007). Crystal structure of the human beta2 adrenergic G-protein-coupled receptor. *Nature*, **450**, 383–387.
17. Alexandrov, A. I., Mileni, M., Chien, E. Y., Hanson, M. A. & Stevens, R. C. (2008). Microscale fluorescent thermal stability assay for membrane proteins. *Structure*, **16**, 351–359.
18. Magnani, F., Shibata, Y., Serrano-Vega, M. J. & Tate, C. G. (2008). Co-evolving stability and conformational homogeneity of the human adenosine A_{2a} receptor. *Proc. Natl Acad. Sci. USA*, **105**, 10744–10749.
19. Serrano-Vega, M. J., Magnani, F., Shibata, Y. & Tate, C. G. (2008). Conformational thermostabilization of the beta1-adrenergic receptor in a detergent-resistant form. *Proc. Natl Acad. Sci. USA*, **105**, 877–882.
20. Weiss, H. M. & Grisshammer, R. (2002). Purification and characterization of the human adenosine A(2a) receptor functionally expressed in *Escherichia coli*. *Eur. J. Biochem.* **269**, 82–92.
21. Murakami, M. & Kouyama, T. (2008). Crystal structure of squid rhodopsin. *Nature*, **453**, 363–367.
22. Park, J. H., Scheerer, P., Hofmann, K. P., Choe, H. W. & Ernst, O. P. (2008). Crystal structure of the ligand-free G-protein-coupled receptor opsin. *Nature*, **454**, 183–187.
23. Scheerer, P., Park, J. H., Hildebrand, P. W., Kim, Y. J., Krauss, N., Choe, H. W. *et al.* (2008). Crystal structure of opsin in its G-protein-interacting conformation. *Nature*, **455**, 497–502.

24. Kobilka, B. K. & Deupi, X. (2007). Conformational complexity of G-protein-coupled receptors. *Trends Pharmacol. Sci.* **28**, 397–406.
25. Tanaka, K., Masu, M. & Nakanishi, S. (1990). Structure and functional expression of the cloned rat neurotensin receptor. *Neuron*, **4**, 847–854.
26. Luca, S., White, J. F., Sohal, A. K., Filippov, D. V., van Boom, J. H., Grisshammer, R. & Baldus, M. (2003). The conformation of neurotensin bound to its G protein-coupled receptor. *Proc. Natl Acad. Sci. USA*, **100**, 10706–10711.
27. Barroso, S., Richard, F., Nicolas-Ethève, D., Reversat, J. L., Bernassau, J. M., Kitabgi, P. & Labbé-Jullié, C. (2000). Identification of residues involved in neurotensin binding and modeling of the agonist binding site in neurotensin receptor 1. *J. Biol. Chem.* **275**, 328–336.
28. Richard, F., Barroso, S., Nicolas-Ethève, D., Kitabgi, P. & Labbè-Julliè, C. (2001). Impaired G protein coupling of the neurotensin receptor 1 by mutations in extracellular loop 3. *Eur. J. Pharmacol.* **433**, 63–71.
29. Kitabgi, P. (2002). Targeting neurotensin receptors with agonists and antagonists for therapeutic purposes. *Curr. Opin. Drug Discov. Dev.* **5**, 764–776.
30. White, J. F., Trinh, L. B., Shiloach, J. & Grisshammer, R. (2004). Automated large-scale purification of a G protein-coupled receptor for neurotensin. *FEBS Lett.* **564**, 289–293.
31. Lau, F. W., Nauli, S., Zhou, Y. & Bowie, J. U. (1999). Changing single side-chains can greatly enhance the resistance of a membrane protein to irreversible inactivation. *J. Mol. Biol.* **290**, 559–564.
32. Zhou, Y. & Bowie, J. U. (2000). Building a thermostable membrane protein. *J. Biol. Chem.* **275**, 6975–6979.
33. Tucker, J. & Grisshammer, R. (1996). Purification of a rat neurotensin receptor expressed in *Escherichia coli*. *Biochem. J.* **317**, 891–899.
34. Martin, S., Botto, J. M., Vincent, J. P. & Mazella, J. (1999). Pivotal role of an aspartate residue in sodium sensitivity and coupling to G proteins of neurotensin receptors. *Mol. Pharmacol.* **55**, 210–215.
35. Zsurger, N., Mazella, J. & Vincent, J. P. (1994). Solubilization and purification of a high affinity neurotensin receptor from newborn human brain. *Brain Res.* **639**, 245–252.
36. Ballesteros, J. A. & Weinstein, H. (1995). Integrated methods for the construction of three-dimensional models and computational probing of structure–function relations in G protein-coupled receptors. In *Methods in Neurosciences, Receptor Molecular Biology* (Sealfon, S. C., ed), vol. 25, pp. Academic Press, New York.
37. Schwartz, T. W., Frimurer, T. M., Holst, B., Rosenkilde, M. M. & Elling, C. E. (2006). Molecular mechanism of 7TM receptor activation—a global toggle switch model. *Annu. Rev. Pharmacol. Toxicol.* **46**, 481–519.
38. Kitabgi, P. (2006). Functional domains of the subtype 1 neurotensin receptor (NTS1). *Peptides*, **27**, 2461–2468.
39. Pang, Y. P., Cusack, B., Groshan, K. & Richelson, E. (1996). Proposed ligand binding site of the transmembrane receptor for neurotensin(8–13). *J. Biol. Chem.* **271**, 15060–15068.
40. Labbé-Jullié, C., Barroso, S., Nicolas-Etève, D., Reversat, J. L., Botto, J. M., Mazella, J. *et al.* (1998). Mutagenesis and modeling of the neurotensin receptor NTR1. Identification of residues that are critical for binding SR 48692, a nonpeptide neurotensin antagonist. *J. Biol. Chem.* **273**, 16351–16357.
41. Barroso, S., Richard, F., Nicolas-Ethève, D., Kitabgi, P. & Labbé-Jullié, C. (2002). Constitutive activation of the neurotensin receptor 1 by mutation of Phe(358) in helix seven. *Br. J. Pharmacol.* **135**, 997–1002.
42. Vogel, R., Mahalingam, M., Ludeke, S., Huber, T., Siebert, F. & Sakmar, T. P. (2008). Functional role of the "ionic lock"—an interhelical hydrogen-bond network in family A heptahelical receptors. *J. Mol. Biol.* **380**, 648–655.
43. Sarkar, C. A., Dodevski, I., Kenig, M., Dudli, S., Mohr, A., Hermans, E. & Plückthun, A. (2008). Directed evolution of a G protein-coupled receptor for expression, stability, and binding selectivity. *Proc. Natl Acad. Sci. USA*, **105**, 14808–14813.
44. Gully, D., Labeeuw, B., Boigegrain, R., Oury-Donat, F., Bachy, A., Poncelet, M. *et al.* (1997). Biochemical and pharmacological activities of SR 142948A, a new potent neurotensin receptor antagonist. *J. Pharmacol. Exp. Ther.* **280**, 802–812.
45. Grisshammer, R. & Tucker, J. (1997). Quantitative evaluation of neurotensin receptor purification by immobilized metal affinity chromatography. *Protein Expression Purif.* **11**, 53–60.
46. Hellmich, M. R., Battey, J. F. & Northup, J. K. (1997). Selective reconstitution of gastrin-releasing peptide receptor with G alpha q. *Proc. Natl Acad. Sci. USA*, **94**, 751–756.
47. Hartman, J. I. & Northup, J. K. (1996). Functional reconstitution in situ of 5-hydroxytryptamine2c (5HT2c) receptors with alphaq and inverse agonism of 5HT2c receptor antagonists. *J. Biol. Chem.* **271**, 22591–22597.
48. Jian, X., Sainz, E., Clark, W. A., Jensen, R. T., Battey, J. F. & Northup, J. K. (1999). The bombesin receptor subtypes have distinct G protein specificities. *J. Biol. Chem.* **274**, 11573–11581.
49. Fawzi, A. B., Fay, D. S., Murphy, E. A., Tamir, H., Erdos, J. J. & Northup, J. K. (1991). Rhodopsin and the retinal G-protein distinguish among G-protein beta gamma subunit forms. *J. Biol. Chem.* **266**, 12194–12200.
50. Gully, D., Canton, M., Boigegrain, R., Jeanjean, F., Molimard, J. C., Poncelet, M. *et al.* (1993). Biochemical and pharmacological profile of a potent and selective nonpeptide antagonist of the neurotensin receptor. *Proc. Natl Acad. Sci. USA*, **90**, 65–69.